TAO, Vol. 8, No. 4, 405-426, December 1997

Aquatic Chemistry of Lakes and Reservoirs in Taiwan

Yuan-Hui Li[1], Chen-Tung A. Chen[2] and Jia-Jang Hung[2]

(Manuscript received 26 June 1997, in final form 30 October 1997)

ABSTRACT

The composition of lake and reservoir waters in Taiwan is mainly controlled by inputs from chemical weathering and by concentration through water evaporation. Inputs from seasalt aerosols are secondary. Sulfate in the water samples mostly originates from oxidation of sulfide minerals in source rocks, such as marbles, gneiss and schists, in the Central Range of Taiwan. Pco_2 values estimated from pH and alkalinity data are mostly higher than the atmospheric Pco_2, indicating a net input of CO_2 from biological respiration over photosynthesis in lakes and reservoirs. Those water samples are also undersaturated with respect to calcite. Some coastal water samples with high alkalinity have unusually high pH (or low Pco_2) and are saturated or slightly oversaturated with respect to calcite, probably suggesting a net removal of CO_2 by active photosynthesis along with evaporative concentration of alkalinity in these water bodies. Some high mountain lakes are low in alkalinity and may be susceptible to acidification by acid rain. However, exceptionally high chemical weathering rates in the Central Range may mitigate the acid rain problem. Kaolinite is a stable secondary mineral in high mountain lakes (>2000 m), whereas Ca-smectite and/or kaolinite are stable secondary minerals in other water bodies. The chemical weathering rates of the Taiwan Island are extremely high, but the chemical compositions of lakes and reservoirs in Taiwan are, in general, similar to the composition of the world mean river water.

(Key words: Lakes, Reservoirs, Major ions, Seasalt, Microbial oxidation, Chemical weathering, Calcite saturation)

1. INTRODUCTION

The island of Taiwan has a length of 385 km, a maximum width of 143 km and a total area of 36,000 km^2. The Central Range is the backbone of the island (Figure 1) and has more than 25 mountain peaks with altitudes exceeding 3000 m. The highest mountain, Mt.Yueshan, is

[1]Department of Oceanography, University of Hawaii, Honolulu, Hawaii 96822 USA
[2]Institute of Marine Geology, National Sun Yat-Sen University, Kaohsiung, Taiwan, ROC

3997 m above sea level. Taiwan is situated on the collision boundary between the Eurasian and the Philippine Sea plates and thus has been very active geotectonically since its formation in the late Paleozoic to Mesozoic. Age-dating of raised coral reefs and fossil shells (Konishi *et al*, 1968: Peng *et al*, 1977; Liew *et al*, 1990; Wang and Burnett, 1990) and the measurement of the elevation changes of benchmarks by geodetic leveling (Liu and Yu, 1990) all indicate rapid uplift rates (mostly in the range of 2 to 10 mm/yr but sometime as high as 35 mm/yr in some places) of the island from the early Holocene to the present. The high uplift rate and high relief of the island result in the observed rapid physical and chemical weathering rates of the Central Range today (1300 mg/cm^2 yr and 65 mg/cm^2 yr, respectively; Li, 1976).

The composition of river and lake waters often reflect the chemical weathering processes in the upstream drainage areas. Factors controlling the chemistry of river and lake waters are summarized by Drever (1985,1988), Stumm (1985), Meybeck (1987a, 1987b) and Lerman *et al.* (1995). Many case studies are also summarized by Degens (1982) and Degens *et al.* (1983, 1985). The case study of the Amazon River by Stallard and Edmond (1981,1983 and 1987) is one outstanding recent example. They demonstrated the importance of precipitation inputs, the influence of geology and the weathering environment as well as the thermodynamic constraints on the chemistry of the Amazon River waters.

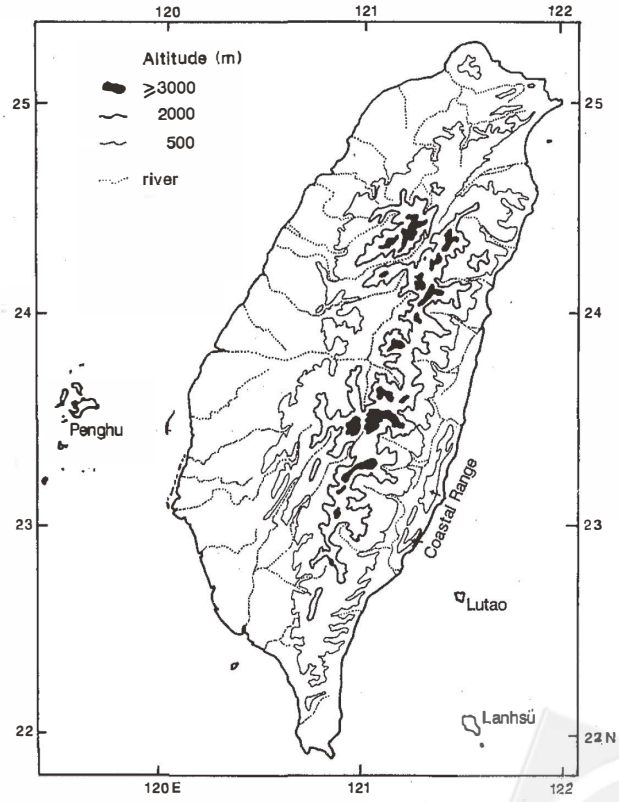

Fig. 1. Topographic map of Taiwan (modified after Wang, 1980).

In this paper, some chemical composition data of lakes and reservoir waters in Taiwan are presented. The objectives are (1) to illustrate spatial variation in the water chemistry of lakes and reservoirs in Taiwan; (2) to show the relationships among the concentrations of major cations and anions; (3) to elucidate factors controlling the chemistry of water samples, such as seasalt and rainwater inputs, chemical weathering of surficial rocks, chemical equilibria, biological activities and evaporation; (4) to evaluate the susceptibility of lakes and reservoirs to acidification by acid rain; and (5) to compare the compositions with those of world-wide surface waters so as to detect any significant differences.

Because rainfall and its subsequent evaporation provide important background information, the contour maps of the average annual precipitation and evaporation rates of water (in cm/yr) over Taiwan are given in Figures 2a and 2b for reference (modified after the Central Weather Bureau, 1991; and Wang and Yi, 1992). In general, the Central Range and the northeastern coast report high precipitation, mainly as a result of typhoons and monsoons. The highest precipitation rate is 480 to 500 cm/yr in northeastern Taiwan. In contrast, the western coastal area is low in precipitation but high in evaporation. In some areas, especially in the most western parts of Taiwan and the Penghu Islands, the evaporation exceeds the precipitation (compare Figs. 2a and 2b).

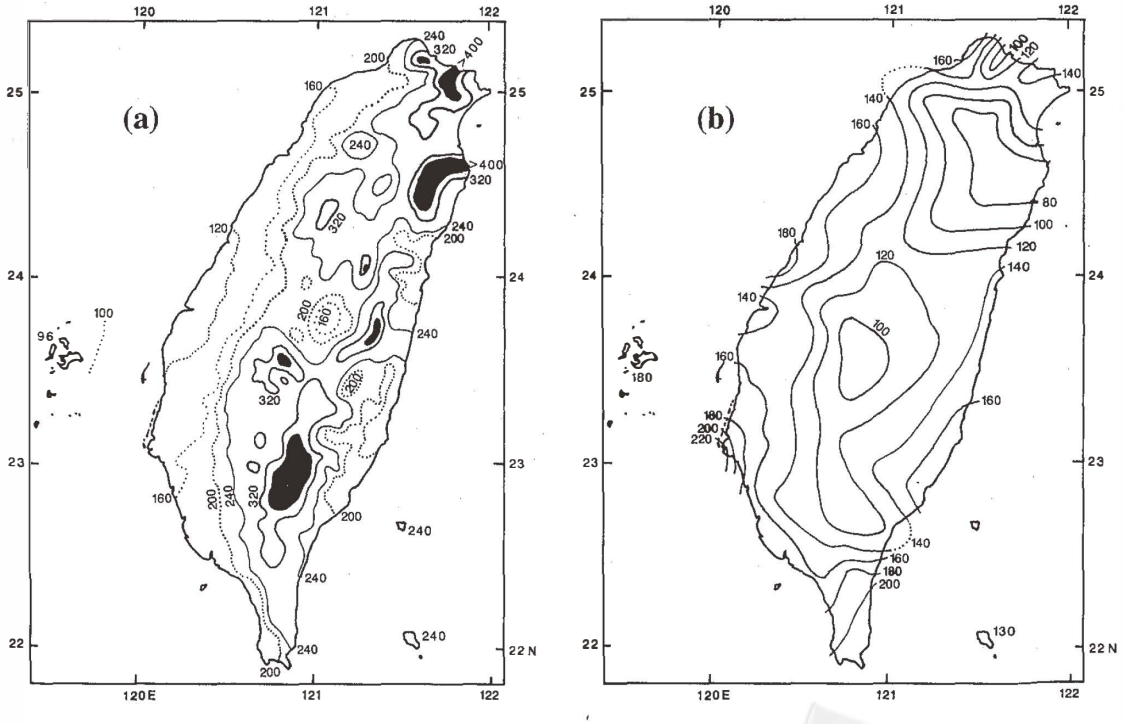

Fig. 2. Contour maps of (a) annual precipitation rates (modified after the Central Weather Bureau, 1991), and (b) annual evaporation rate over Taiwan (modified after Wang and Yi, 1992).

2. SAMPLING AND ANALYTICAL METHODS

Water samples from lakes and reservoirs were collected with plastic buckets and a Hydro-Bios water sampler, usually from the top two meters at two different locations within each water body. The temperature and pH of water samples were measured immediately in the field. Samples were filtered with 0.45 mm Nalgene filters, stored in amber plastic bottles at 4°C and then shipped back to the laboratory for chemical analysis.

The 4.004 and 7.415 pH buffers from the National Institute of Standard and Technology (NIST) USA were adopted to calibrate the Radiometer PHM 85 system. The reproducibility is within ± 0.003 pH units. Alkalinity was measured with the Gran Titration. The concentrations of K^+, Na^+, NH_4^+, Ca^{+2}, Mg^{+2}, Cl^-, NO_3^- and SO_4^{-2} were analyzed by a Dionex 2000i Ion Chromatograph. A Perkin Elmer 2380 AA provided additional analysis for Ca^{+2}, Mg^{+2}, K^+ and Na^+. Certified rainwater standard samples (2694I and 2694II) supplied by the Environmental Resource Associate (ERA) were used as references. The overall analytical error is equal to or less than 6 %. The details of those analytical methods are given elsewhere (Chen *et al.*, 1988, 1994).

3. RESULTS AND DISCUSSION

3.1 Data

More than 600 water samples from about 120 lakes and reservoirs throughout Taiwan were analyzed (Chen *et al.*, 1988; Chen, 1994). From these we have selected one representative sample for each lake and reservoir. Each selected sample is internally consistent with regard to the charge balance between major cations and anions (*i.e.*, the total cationic and anionic charge ratio in the range of 1.0 ± 0.3). The chemical compositions of those selected water samples are summarized in Table 1, and sampling locations are shown in Figure 3. All are expressed in meq/l unless noted otherwise. Readers may contact the authors for the individual names of lakes and reservoirs. The so-called mountain samples in Figure3 (solid circles = m) were obtained from water bodies at altitude greater than 500 m. For ease of identification, water samples from coastal areas less than 500 m in altitudes are further grouped into north (open circles = n), south (open triangles = s), and east (open squares = e) along with four offshore island samples (crosses = i).

In addition to the charge balance, the degree of agreement between measured conductivity (k_{obs}) and calculated conductivity (k_{cal}) provides an additional check on the internal consistency of the data set given in Table 1. The k_{cal} (in μS/cm) can be obtained by the equation:

$$k_{cal} = \Sigma U_i m_i |Z_i| ,$$

where U_i = mobility of ion i (cm^2/ohm/equivalent); m_i = concentration of ion i (μmol/cm^3); $|Z_i|$ = absolute value of ion charge; and μS = 10^{-6} ohm^{-1}. The U_i values for cations and anions in infinitely diluted solutions at 25°C were obtained from the Handbook of Chemistry and Physics (CRC Press, 1994). As shown in Figure 4, the general agreement between k_{obs} and k_{cal} values is excellent, except for a few samples with low conductivity where the accurate mea-

Table 1: Chemical compositions of water samples from Taiwan's lakes and reservoirs. The concentrations of major ions and alkallinity (Alk) are in the unit of meq/l.

Sample	HEIGHT (m)	PH	k (μS/cm)	ALK	SO4	NO3	CL	CA	MG	K	NA	Z+/Z-	k(cal)/k
North (n)													
1	150	6.63	92	0.049	0.159	0.014	0.477	0.062	0.138	0.025	0.529	1.08	1.00
3	<50	6.90	112	0.527	0.275	0.035	0.340	0.098	0.267	0.024	0.686	0.92	1.16
4	70	7.46	117	0.417	0.345	0.029	0.341	0.127	0.267	0.027	0.738	1.02	1.15
5	10	8.06	263	1.449	0.841		0.275	0.902	1.007	0.053	0.401	0.92	1.07
6	<50	6.98	130	0.715	0.248	0.025	0.257	0.296	0.253	0.043	0.361	0.77	0.96
7	65	7.67	76	0.264	0.160	0.010	0.219	0.140	0.144	0.019	0.334	0.98	1.00
8	45	6.97	83	0.351	0.222		0.137	0.295	0.183	0.029	0.164	0.95	0.99
9	10	6.97	101	0.459	0.254	0.018	0.188	0.177	0.204	0.038	0.294	0.78	0.94
10	<50	6.55	200	1.264	0.224	0.003	0.446	0.881	0.208	0.094	0.588	0.91	1.04
11	10	7.15	125	0.572	0.272	0.017	0.273	0.270	0.187	0.062	0.346	0.76	0.94
12	20	7.40	95	0.610	0.288	0.021	0.085	0.531	0.261	0.018	0.231	1.04	1.23
13	160	6.96	79	0.450	0.242	0.016	0.130	0.275	0.252	0.018	0.257	0.96	1.20
14	30	8.20	92	0.590	0.292	0.016	0.073	0.500	0.266	0.016	0.214	1.03	1.22
15	50	7.68	194	0.545	0.809		0.371	0.559	0.390	0.084	0.669	0.99	1.09
16	386	7.17	71	0.403	0.064		0.139	0.301	0.074	0.079	0.148	0.99	0.97
17	220	7.24	85	0.248	0.227		0.223	0.221	0.138	0.072	0.266	1.00	1.01
18	250	7.75	136	0.815	0.271	0.014	0.140	0.587	0.228	0.035	0.336	0.96	1.00
19	<50	7.59	258	0.826	0.789	0.012	0.575	1.014	0.239	0.184	0.775	1.00	1.05
20	240	8.91	136	0.900	0.392	0.022	0.034	0.817	0.520	0.020	0.074	1.06	1.15
21	36	7.69	510	3.767	0.704	0.033	0.701	2.324	1.474	0.194	1.204	1.00	1.12
22	141	8.57	115	0.730	0.314	0.003	0.152	0.519	0.417	0.104	0.219	1.05	1.23
23	50	9.16	186	1.399	0.361	0.128	0.133	0.958	0.577	0.042	0.430	0.99	1.20
24	70	8.60	235	1.184	0.613	0.036	0.125	1.210	0.540	0.048	0.250	1.05	0.98
25	60	8.40	230	1.350	0.203	0.054	0.094	1.030	0.470	0.028	0.180	1.00	0.80
26	242	8.93	305	2.010	0.626	0.321	0.192	1.788	1.175	0.082	0.866	1.24	1.30
27	270	8.23	182	1.288	0.452	0.055	0.049	0.955	0.553	0.020	0.236	0.96	1.10
Ave.		7.69	156	0.794	0.371	0.042	0.237	0.648	0.401	0.056	0.415	0.98	1.07
South (s)													
1	97	7.76	339	1.690	1.287	0.070	0.400	0.513	1.952	0.072	0.431	0.86	1.11
2	50	9.38	303	1.481	1.372		0.271	1.052	0.995	0.049	0.594	0.86	1.14
3	17	10.33	331	2.054	0.678	0.029	0.522	0.384	0.305	0.255	1.975	0.89	1.04
4	17	7.76	668	4.470	1.810	0.013	0.968	1.988	1.576	0.087	2.561	0.86	1.13
5	85	7.16	230	1.320	0.092	0.304	0.500	0.127	0.525	0.096	1.144	0.85	0.98
6	20	7.93	761	6.747	1.196	0.039	1.407	3.583	2.085	0.072	1.995	0.82	1.23
7	23	9.21	(314)	1.622	0.234	0.003	0.745	0.731	0.478	0.413	1.348	1.13	
8	20	8.31	(744)	2.221	1.622	0.032	2.125	1.915	1.307	0.435	2.724	1.06	
9	80	8.50	360	2.740	0.524	0.060	0.163	1.640	1.100	0.057	0.860	1.05	1.07
10	100	8.51	405	2.980	0.486	0.050	0.479	1.840	1.060	0.056	1.300	1.07	1.10
12	200	8.07	260	1.930	0.029	0.150	0.043	1.510	0.750	0.043	0.310	1.21	0.96
13	50	8.56	270	2.040	0.290	0.110	0.067	1.400	0.760	0.033	0.380	1.03	1.01
14	15	7.95	788	3.930	1.080	0.015	3.360	1.860	0.920	0.240	3.178	0.74	1.09
15	380	6.85	613	3.275	1.982	0.064	0.518	3.917	0.566	0.263	0.263	0.85	1.05
16	<50	7.97	324	2.110	0.844	0.003	0.312	1.300	1.750	0.060	0.751	1.18	1.23
17	45	7.34	400	2.940	0.886	0.030	0.253	2.300	1.003	0.110	0.144	0.87	1.07
18	180		244	1.720	1.153	0.023	0.039	2.206	0.837	0.017	0.375	1.17	1.51
19	35	8.71	350	2.800	0.339	0.130	0.480	1.920	1.080	0.174	0.790	1.06	1.20
20	<50	7.08	187	1.740	0.010	0.010	0.115	0.837	0.501	0.048	0.472	0.99	1.02
21	130	7.43	420	2.550	1.600		0.029	2.260	0.993	0.017	0.378	0.87	1.07
22	<50	8.46	300	2.090	1.300	0.025	0.507	1.800	0.928	0.159	1.217	1.05	1.56
24	20	8.21	195	1.480	0.800	0.003	0.220	1.375	0.075	0.072	1.087	1.04	1.50
25	50	7.73	285	1.900	0.980	0.093	0.439	2.250	0.933	0.078	0.826	1.20	1.52
27	319	6.65	112	0.065	0.092	0.003	0.780	0.068	0.117	0.033	0.727	1.01	1.06
28	15	7.87	320	2.015	0.499	0.033	0.278	1.656	0.552	0.089	0.810	1.10	1.03
29	<50	7.11	637	2.390	0.468	0.042	1.801	1.216	1.100	0.550	1.727	0.98	0.85
30	<50	7.43	694	5.650	0.047	0.177	1.028	5.239	0.610	0.027	0.853	0.97	1.06
ave.		8.01	363	2.517	0.804	0.060	0.661	1.737	0.921	0.134	1.082	0.99	1.14
Island (i)													
1	10	8.21	1120	3.074	0.816	0.003	7.119	1.347	2.290	0.173	6.209	0.91	1.14
2	60	7.92	504	2.820	0.719	0.443	0.903	3.244	0.303	0.040	0.928	0.92	1.08
3	10	7.71	495	1.687	0.228		1.400	0.494	0.666	0.086	2.045	0.99	0.76
4	330	6.61	65	0.126	0.100	0.003	0.426	0.189	0.126	0.051	0.290	1.00	1.27

East (e)													
1	10	8.87	107	0.815	0.079	0.007	0.173	0.383	0.373	0.018	0.378	1.07	1.11
2	10	8.46	120	0.849	0.187	0.035	0.126	0.537	0.319	0.013	0.358	1.03	1.11
3	165	7.67	370	2.550	1.370	0.026	0.022	1.720	1.536	0.037	0.583	0.98	1.20
4	50	7.65	114	0.437	0.534	0.003	0.061	0.383	0.500	0.020	0.219	1.08	1.13
5	135	6.76	55	0.282	0.044	0.003	0.113	0.148	0.118	0.011	0.193	1.06	0.92
6	<50	7.40	478	2.120	2.510	0.003	0.096	2.690	1.290	0.032	0.228	0.90	1.14
7	170	8.39	426	2.132	2.086	0.003	0.034	2.587	1.124	0.031	0.210	0.93	1.15
ave.		7.89	239	1.312	0.973	0.011	0.089	1.207	0.751	0.023	0.310	1.01	1.11
Mountain (m)													
1	840	6.46	82	0.066	0.073	0.010	0.188	0.102	0.092	0.015	0.205	1.23	0.56
2	865	4.51	41		0.120	0.011	0.113	0.030	0.039	0.020	0.114	0.96	0.99
3	465	6.09	17	0.038	0.027		0.041	0.022	0.032	0.008	0.047	1.04	0.80
4	1230	4.98	7	0.005	0.028	0.008	0.029	0.022	0.007	0.004	0.023	0.95	1.72
5	1140	5.84	11	0.015	0.041	0.003	0.008	0.033	0.017	0.003	0.019	1.10	0.87
6	1670	6.58	25	0.120	0.051		0.015	0.049	0.082	0.006	0.021	0.85	0.78
9	1800	7.48	261	1.658	0.868	0.131	0.030	1.339	0.762	0.018	0.145	0.84	1.09
10	2580	7.48	37	0.283	0.015	0.003	0.035	0.206	0.011	0.011	0.031	0.77	0.86
11	1400	8.57	173	1.269	0.486	0.015	0.027	0.905	0.612	0.012	0.240	0.98	1.14
12	940	7.73	181	1.345	0.475	0.037	0.026	1.005	0.591	0.013	0.202	0.96	1.13
13	2940	5.81	7	0.010	0.009	0.003	0.009	0.007	0.010	0.007	0.004	0.95	0.61
15	1700	8.44	137	1.093	0.248	0.013	0.008	0.611	0.368	0.012	0.070	0.78	0.95
16	720	6.65	15	0.153	0.019	0.002	0.096	0.112	0.039	0.034	0.031	0.80	1.96
17	530	7.36	61	0.390	0.152	0.066	0.051	0.220	0.190	0.018	0.165	0.90	1.16
19	945	8.28	255	1.920	0.776	0.021	0.018	1.155	1.005	0.016	0.386	0.94	1.15
22	740	8.20	300	2.072	1.077	0.024	0.015	1.897	1.128	0.032	0.340	1.07	1.24
23	2870	5.64	4	0.003	0.019		0.021	0.017	0.010	0.007	0.013	0.89	1.93
24	1160	7.54	137	1.056	0.150	0.049	0.049	0.668	0.296	0.023	0.195	0.91	0.97
25	1800	7.33	95	0.646	0.098	0.009	0.062	0.469	0.165	0.023	0.189	1.04	0.95
26	2100	7.47	84	0.300	0.124	0.151	0.046	0.397	0.143	0.014	0.089	1.04	0.88
27	2100	7.55	105	0.380	0.196	0.172	0.057	0.503	0.212	0.015	0.121	1.06	0.93
28	2100	7.82	183	1.200	0.122	0.009	0.035	1.160	0.464	0.031	0.045	1.24	0.90
30	2335	5.90	15	0.014	0.014	0.003		0.006	0.003	0.004	0.014	0.91	
32	2150	8.50	103	0.702	0.251	0.003	0.019	0.578	0.337	0.005	0.078	0.94	1.06
33	2150	6.41	6	0.017	0.009	0.003	0.008	0.004	0.006	0.005	0.017	0.88	0.66
34	2040	6.40	31	0.162	0.013	0.006	0.073	0.146	0.025	0.009	0.100	1.10	0.97
ave.		6.96	91	0.597	0.210	0.033	0.043	0.449	0.256	0.014	0.112	0.97	1.05
World mean river				0.869	0.240		0.233	0.734	0.300	0.036	0.313	1.03	

	PH	NH4	SO4	NO3	CL	CA	MG	K	NA	Z+/Z-
Rainwater										
Taipei	4.15	0.049	0.119	0.043	0.148	0.077	0.026	0.025	0.101	1.12
ave.Taiwan	4.45	0.039	0.101	0.029	0.146	0.046	0.032	0.033	0.115	1.11

surements of both conductivity and ionic concentrations were less precise.

As shown in the ternary diagram of alkalinity-SO_4- Cl data (Figure 5a), alkalinity accounts for more than 50 % of the total anions for most samples, as is also the case for the world mean river water (the large open circle in Figure 5a; Meybeck, 1987a, b). Chloride is predominant only in a few coastal samples (i1, i4, m1, e1 and s27). For samples m2, m5, e4 and e5, more than 50 % of the total anions is SO_4 (Figure 5a).

Figure 5b illustrsates the ternary diagram of non-seasalt major cations (ns-Ca, ns-Mg and ns-Na) after the seasalt contributions were subtracted by assuming that all Cl is of seasalt origin, *i.e.*, ns-X = X - Cl * $(X/Cl)_{seawater}$, where X and Cl are the concentrations of a given cation and chloride in a sample respectively, while $(X/Cl)_{seawater}$ is the ratio in seawater. The ns-Ca accounts for more than 50 % of the total non-seasalt cations for two-thirds of the samples, just as in the case of the world mean river water (the large open circle in Figure 5b). The predominance of ns-Na in samples n1, n3, n4, ,s3, s5, s27, m30 and m33 (Figure 5b) may indicate Na inputs from the chemical weathering of surficial rocks high in feldspars and Na-plagioclase. In comparison with the mean composition of Taiwan's upper crust (the large open star in Figure 5b; Lan *et al.*, 1991), Ca is preferentially leached out over Mg, Mg over Na,

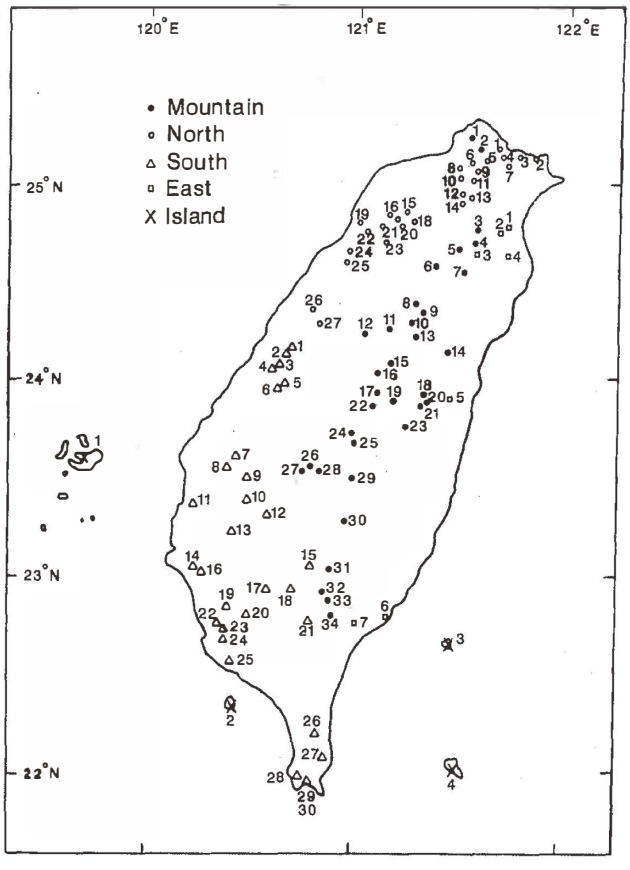

Fig. 3. (a) Localities of lakes and reservoirs in mountain (>500 m, solid circles), coastal areas (north, open circles; south, open triangles; east, open squares), and offshore islands (crosses). The symbols remain the same in all of the following figures.

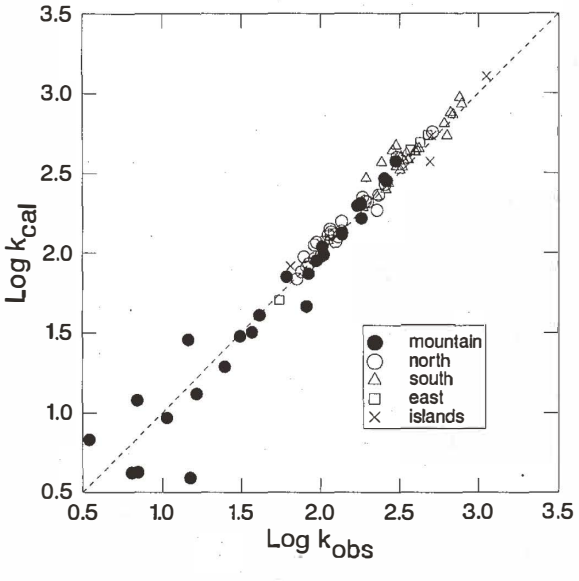

Fig. 4. Comparison of the observed and calculated conductivities for lake and reservoir waters. The dotted diagonal line represents the concordant line.

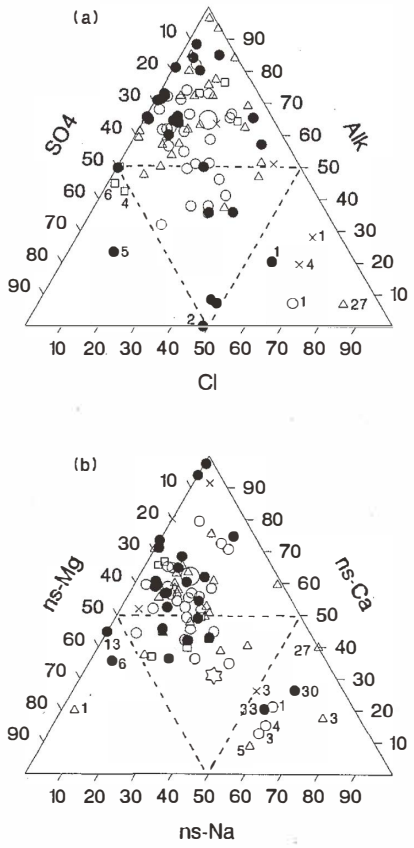

Fig. 5. Ternary diagrams of (a) alkalinity, SO_4 and Cl data and (b) non-seasalt Ca, Mg and Na of Taiwan's lake and reservoir waters. The large open circles represent the data for the world mean river water (Meybeck, 1987a and b). The large open star represents the data point for the average crust rocks of Taiwan (Lan *et al.*, 1991), which is very similar to the world's average upper crust. Numerals are specific sample numbers given in Table 1.

and as is discussed later Na over K by the water samples (except for the ns-Na dominant samples), again this is also the case for the world mean river water. It was noted that the mean composition of Taiwan's upper crust is very similar to that of the world average (Lan *et al.*, 1991).

3.2 Spatial Distribution Patterns of Major Ion Concentrations

The isopleth maps for chlorine (Cl), alkalinity (Alk) and sulfate (SO_4), as shown in Figures 6a, 6b and 6c respectively, point out a trend of generally low concentrations of these species in high mountain areas, but high concentrations toward coastal areas, especially those toward the west. Figures 7a to 7d also show the concentration changes in Cl, Alk, SO_4 and Na as a function of the altitude of lakes and reservoirs.

The Cl concentrations in the mountain samples are uniformly low (< 0.05 meq/l;Figure 6a and 7a) when compared to the average rainwater of Taiwan (0.15 meq Cl/l, at the bottom of Table 1; rainwater data are from Chen *et al.*, 1994), whereas alkalinity is high between the altitude 500 and 2300 m (Figure 7c). The implications here are that the seasalt aerosols are the main source of Cl in the samples, and a large fraction of these seasalt aerosols carried by air masses is washed out by rainfall before reaching the high mountain or inland areas (Stallard and Edmond, 1981; Li, 1992). Also, seasalt is diluted by high rainfall in the high mountain

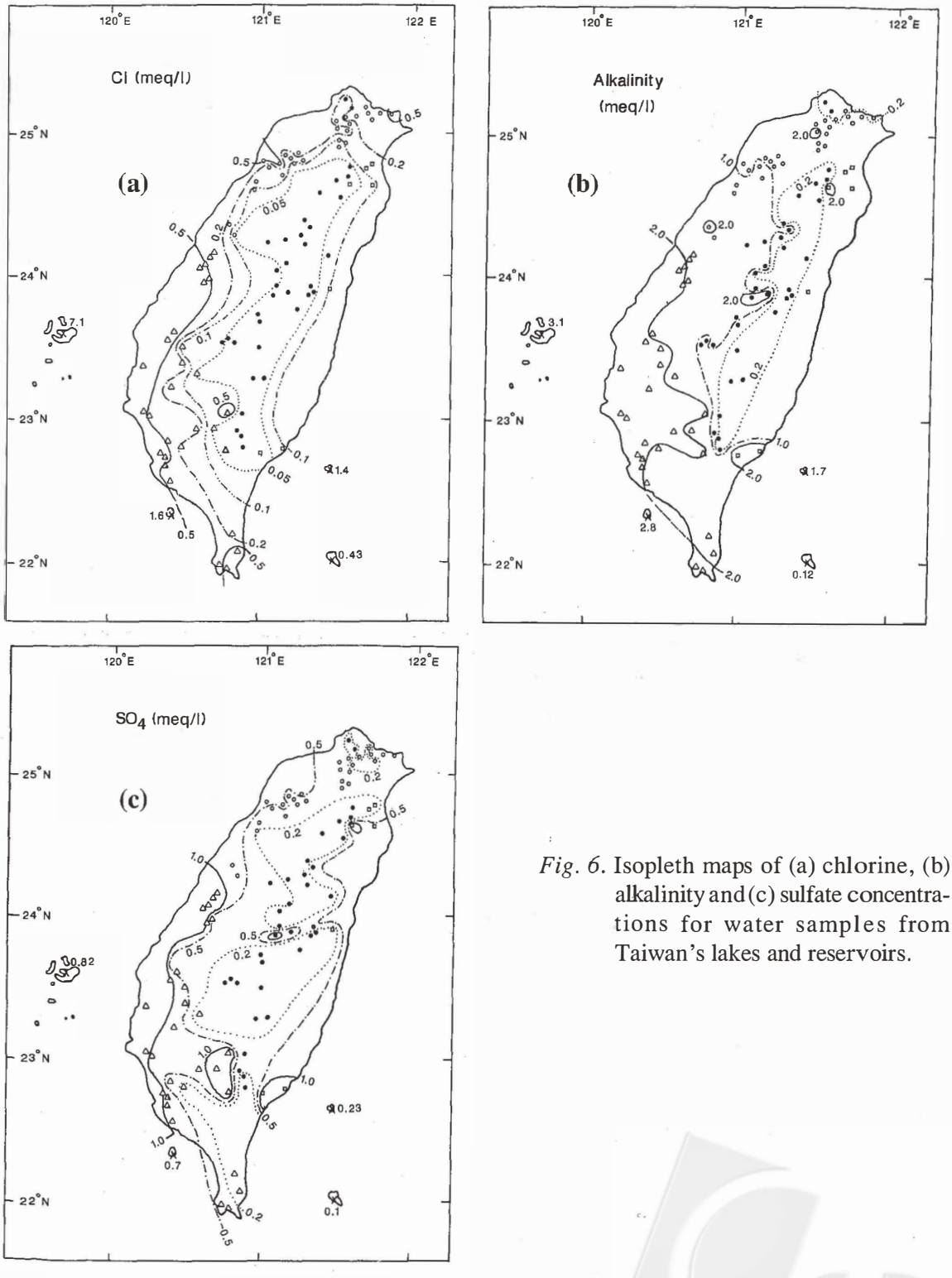

Fig. 6. Isopleth maps of (a) chlorine, (b) alkalinity and (c) sulfate concentrations for water samples from Taiwan's lakes and reservoirs.

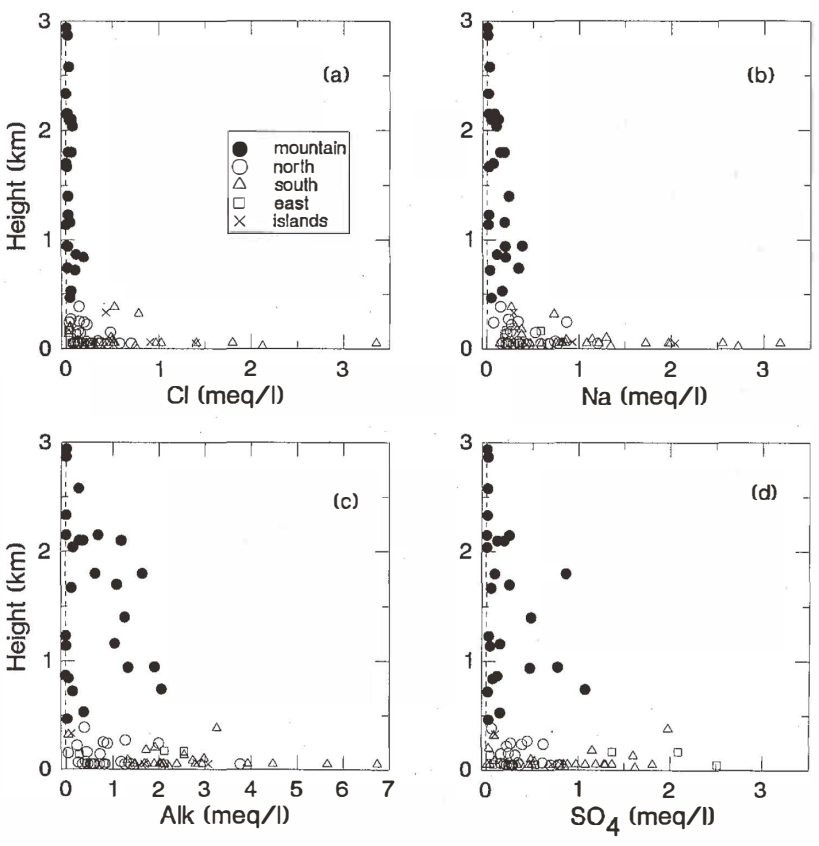

Fig. 7. Plots of altitude versus (a) Cl, (b) Na, (c) Alkalinity, and (d) SO_4 concentrations in lake and reservoir waters.

area. In contrast, the high Cl concentration in the western coastal area (from about 0.5 meq/l to as high as 7.1 meq/l in the Penghu Islands;Figure 6a) indicates the excess amount of evaporation over precipitation (Figure 2a and 2b), and the high inputs of seasalt aerosols and sea sprays.

Alkalinity results from the chemical weathering of aluminosilicate and carbonate rocks. The low alkalinity (< 0.2 meq/l) in some parts of the high mountain area (Figure 6b) is mainly caused by dilution through high rainfall there. The low-alkalinity lakes may be susceptible to acidification by acid rains. However, in view of the extremely high chemical weathering rate in the Central Range (about 65 mg/cm^{2}yr; Li, 1976), acidification of lakes is less likely. For example, the chemical weathering rate of 65 mg/cm^{2}yr roughly corresponds to a consumption rate of 0.5 meq H^+/cm^{2}yr (Li, 1972). The hydrogen ions are mainly provided by oxidation of the organic matter in soils. For comparison, the most polluted rainwater from Taipei (Table 1) can deliver only about 0.01 to 0.02 meq H^+/cm^{2}yr. However, one cannot totally rule out the possibility that the chemical weathering rate in the drainage areas of some high mountain lakes may be low, such that the acidification of lakes by acid rain may become feasible. The drastic increase in alkalinity yet with the constantly low Cl concentration in the mountain

samples (Figures 7a, 7c and 8e) indicates that the increase in alkalinity is mainly caused by intense chemical weathering and not by evaporative concentration. In contrast, high alkalinity samples from the southwestern coast (Figure 6b) suggest additional evaporative concentration.

The sources of SO_4 in the water samples may include inputs from seasalt aerosols, fossil fuel burning, and chemical weathering of sulfur containing minerals, such as chalcopyrite, pyrite, gypsum and others. However, gypsum may be excluded because there are no known evaporite or gypsum outcrops in the Central Range area (only a few secondary gypsum deposits in the southwestern part of Taiwan are known to exist). As shown in Figure 8a, the SO_4/Cl ratio of most samples is much higher than those in seawater and polluted rainwater. Therefore, most sulfates are chemical weathering products. The close correlation between alkalinity and SO_4, as shown in Figure 8d., also provides further proof of this.

3.3 Relationships Among Major Ions

The correlation coefficient matrixes obtained from the raw chemical data (Table 1) and from the seasalt corrected data (*i.e.* non-seasalt components) are summarized in Tables 2a and 2b. The high to moderate correlations among alkalinity, SO_4, Ca, Mg and Na (correlation coefficients $\gamma > 0.5$ in Tables 2a and 2b) are graphically presented in Figure 8d, 8f, 9a, 9b, 9d and 9e. These correlations can be explained by the following schematic weathering reactions of carbonate (marbles, limestones) and aluminosilicate rocks (gneiss and schists) which contain many pyrite veins or grains in the Central Range of Taiwan, as stated earlier (Ho, 1975):

$$MCO_3 + CO_2 + H_2O \rightarrow M^{+2} + 2HCO_3^- \; ; \qquad (1a)$$

$$MSiO_3 + 2CO_2 + H_2O \rightarrow M^{+2} + 2HCO_3^- + SiO_2 \; ; \quad \text{and} \qquad (1b)$$

$$4MCO_3 + FeS_2 + 3.75O_2 + 2.5\,H_2O \rightarrow 4M^{+2} + 2SO_4^{-2} + 4HCO_3^- + FeOOH \; , \qquad (1c)$$

where M is Ca and Mg. According to the above reactions, the equivalents of $Ca^{+2} + Mg^{+2}$ should be balanced by those of $HCO_3^- + SO_4^{-2}$. This is the case for most samples shown in Figure 9c. It is clear that seasalt inputs for Ca, Mg and alkalinity are negligible.

The high to moderate correlations among Cl, Na and K ($\gamma > 0.5$) in Table 2a and weak correlations among Cl, ns-Na and ns-K ($\gamma < 0.4$) in Table 2b are again presented graphically in Figsure 8b, 8c and 9f. The Na/Cl and K/Cl ratios (Figure 8b and 8c) as well as the SO_4/Cl ratios (Figure 8a) of most samples are much greater than those in seawater or in polluted rainwater (dotted lines), thus again demonstrating the importance of the chemical weathering inputs for Na ,K and SO_4. The high SO_4/Cl ratios in the polluted rainwaters as compared to that in seawater (Figure 8a) also indicate additional SO_4 sources other than seasalt in rainwater, such as the oxidation of natural dimethyl sulfide (DMS) and fossil fuel burning. The ns-Ca/ns-Mg ratios of most samples are greater than that of the average upper crust of Taiwan (Figure 9d; Lan et. al., 1991), implying preferential weathering of calcium-rich carbonate rocks over gneiss and schists. The ns-Na/ns-Mg ratios scatter around the average upper crust value of

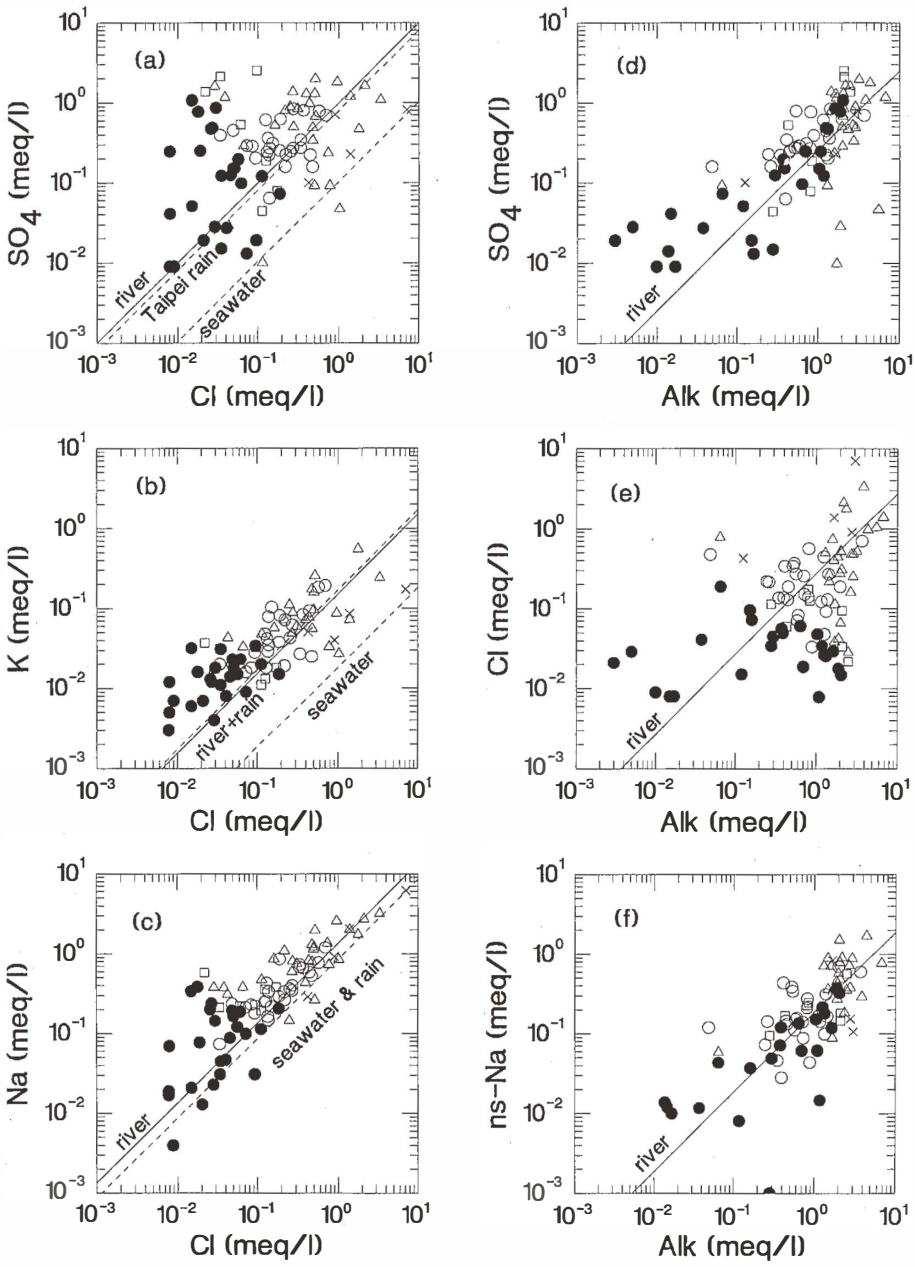

Fig. 8. Correlation plots of various pairs of chemicals. The preface "ns" represents the non-seasalt component. The solid diagonal line in each diagram represents the ratio of a given chemical pair for the world mean river water, while the dotted lines stand for the ratios of seawater and polluted Taipei rainwater.

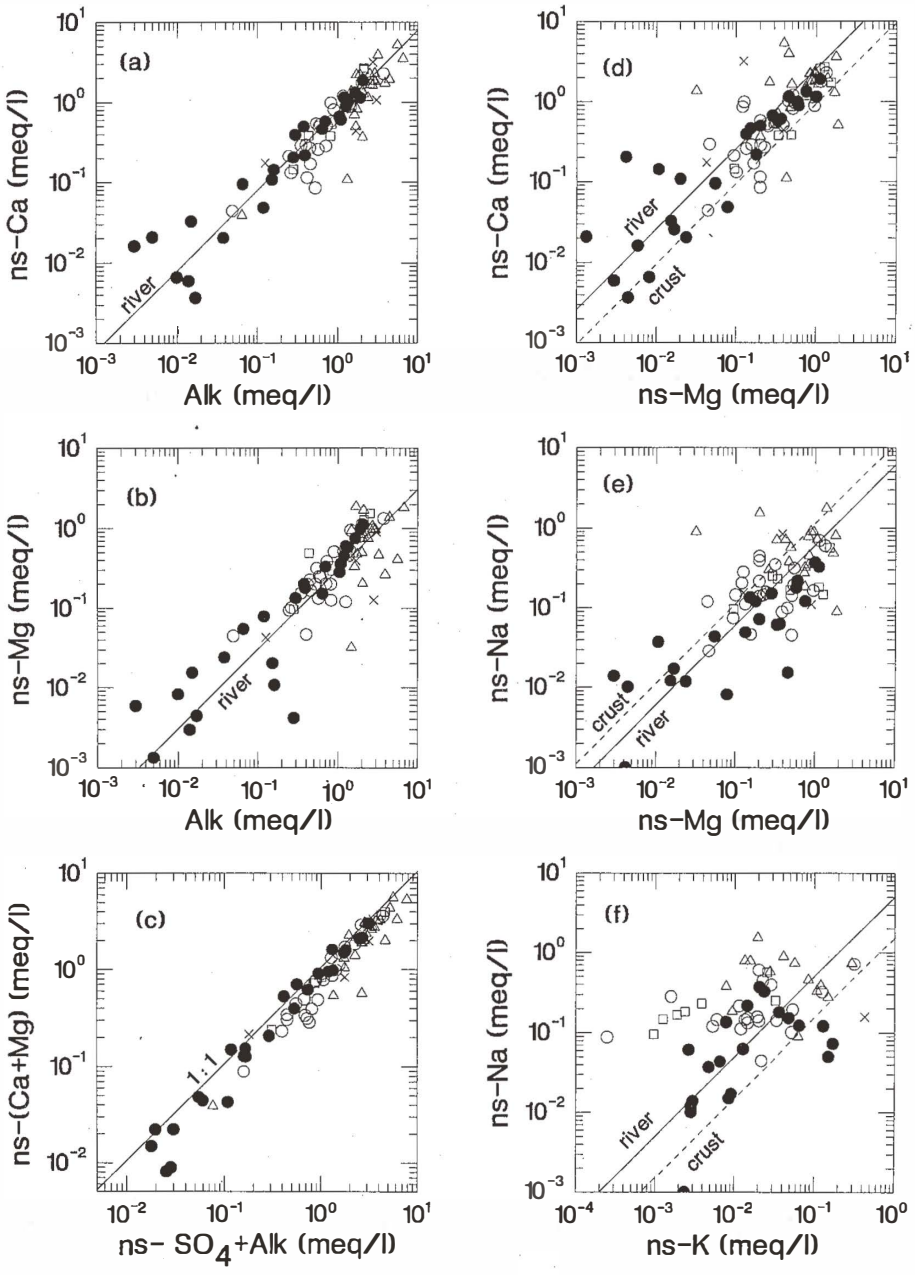

Fig. 9. Correlation plots of various pairs of chemicals. The preface "ns" represents the non-seasalt component. The solid diagonal line in each diagram represents the ratio of a given chemical pair for the world mean river water, and the dotted lines the ratios for the average upper crust of Taiwan.

Table 2: a) Correlation coefficient matrix for raw chemical data (Table 1) from Taiwan's lakes and reservoirs, and b) correlation coefficient matrix for seasalt-corrected data from Table 1.

a)

	Cl	Alk	SO_4	NO_3	Ca	Mg	K	Na	pH
Cl	1.00								
Alk	0.42	1.00							
SO_4	0.21	**0.57**	1.00						
NO_3	-0.01	0.25	-0.02	1.00					
Ca	0.24	**0.88**	**0.63**	0.35	1.00				
Mg	0.48	**0.77**	**0.69**	0.09	**0.61**	1.00			
K	0.48	0.38	0.31	-0.01	0.27	0.34	1.00		
Na	**0.93**	**0.55**	0.32	0.02	0.31	**0.58**	**0.55**	1.00	
pH	0.13	0.42	0.33	0.19	0.43	0.45	0.26	0.29	1.00

b)

	Cl	Alk	ns SO_4	ns-Ca	ns Mg	ns-K	ns-Na
Cl	1.00						
Alk	0.42	1.00					
ns SO_4	0.11	**0.51**	1.00				
ns-Ca	0.37	**0.86**	**0.69**	1.00			
ns Mg	0.27	**0.80**	**0.71**	**0.73**	1.00		
ns-K	0.16	0.22	-0.02	0.30	0.09	1.00	
ns-Na	0.38	**0.61**	0.27	0.38	0.42	0.17	1.00

Taiwan (Figure 9e). The ns-Na/ns-K values are mostly higher than the upper crust value (Figure 9f), indicating preferential mobilization of Na over K during weathering processes as also shown by Colman (1982).

The nitrate concentrations of the samples do not correlate appreciably with any other ion concentrations (Table 2a) and can be lower or higher than the values predicted from rainwater inputs (Figure 10, dotted lines). An NO_3/Cl ratio lower than that of rainwater may indicate an effective removal of nitrate by biological activity, such as photosynthetic uptake and/or microbial denitrification, whereas high nitrate (>0.1 meq/l) samples may indicate serious pollution inputs from fertilizer usage and municipal sewage. Nitrate concentrations greater than 0.02 meq/l may have the potential to give rise to lake eutrophication (Sawyer, 1947). However, Vollenweider (1975) and Schindler (1974, 1977) demonstrated that phosphorus rather than nitrate loading and the mean depth of lake or the mean residence time of lake bottom water concertedly affect lake eutrophication. Lake eutrophication is an important issue which is to be discussed in a separate paper. Only four lake samples exceed the nitrate drinking water standard (0.16 meq/l) recommended by the U. S. Public Health Service (McCabe *et al.*, 1970).

3.4 Carbonate Chemistry and Activity-Activity Diagrams

The partial pressure of CO_2 (Pco_2 in atmospheric units), pH and the activity or concentration of bicarbonate ($[HCO_3^-]$) are related by the following equation (Li, 1988):

$$pH = -\log (K_1 * Pco_2 * Kco_2) + \log [HCO_3^-] \; ; \qquad (2)$$

where $Kco_2 = [H_2CO_3] / Pco_2 = 10^{-1.47}$ and $K_1 = [H^+][HCO_3^-] / [H_2CO_3] = 10^{-6.35}$

Equation 2 is plotted in Figure 11a at different given Pco_2 values. The samples with measured pH and calculated bicarbonate concentrations are also plotted in the same figure. Bicarbonate concentrations were calculated from pH and alkalinity data, where alkalinity was assumed to be equal to carbonate alkalinity. Most samples have Pco_2 values greater than the atmospheric Pco_2 (about $10^{-3.5}$ atm), which is indicative of active microbial oxidation of organic matter in lakes and reservoirs. Some samples with high bicarbonate concentrations have unusually high pH or low predicted Pco_2 values (e.g. s2, s3, s7, n20, n23, n26, e1 in Figure 11a), probably caused by evaporative concentration and active photosynthesis in the water bodies.

If water samples are in equilibrium with calcite, then:

$$\log ([Ca^{+2}] / [H^+]) = \log (Ksp/K_2) - \log [HCO_3^-] , \qquad (3)$$

where $Ksp = [Ca^{+2}] [CO_3^{-2}] = 10^{-8.34}$ and $K_2 = [H^+] [CO_3^{-2}] / [HCO_3^-] = 10^{-10.33}$

K_1, K_2, Ksp, Kco_2 values are taken from Drever (1988). Equation 3 is plotted in Figure 11b as two parallel dotted lines, showing uncertainties in the estimations of Ksp, K_2, and activity coefficients. It is evident from Figure 11b that samples from the high mountain to coastal areas tend to progress systematically from undersaturation to saturation with respect to calcite. Coastal samples with unusually high pH (s2, s3, s7, n20, n23, n26, e1) are also slightly over-saturated with respect to calcite.

The activity-activity ratio diagrams adopted from Drever (1988) are shown in Figure 12a and 12b, and depict the stability fields of Ca-, Mg- and Na-smectites and kaolinite. If lake and reservoir waters are in thermodynamic equilibrium with solid phases, kaolinite is a stable secondary clay mineral in high mountain (> 2000 m) water bodies, whereas Ca-smectite and/or kaolinite are stable secondary clay minerals in other water bodies. However, as emphasized by Drever (1988), thermodynamic equilibrium between solution and clay minerals in natural aquatic environments is rarely attainable.

The tight clustering of water samples along a 1:1 slope in Figure 12a and along a 2:1 slope in Figure 12b, as also shown by Bluth and Kump (1994) in other regions, is probably an artifact and can be explained as follows: $\log ([Ca^{+2}]/[H^+]^2)$ and $\log ([Mg^{+2}]/[H^+]^2)$ are equal to $\log [Ca^{+2}] + 2pH$ and $\log [Mg^{+2}] + 2pH$, where 2pH values for all water samples are always much larger than $\log [Ca^{+2}]$ and $\log [Mg^{+2}]$ values (Table 1). In addition, pH values are roughly proportional to $\log [Ca^{+2}]$ and $\log [Mg^{+2}]$ values (Table 2a). Therefore, both $\log ([Ca^{+2}]/[H^+]^2)$ and $\log ([Mg^{+2}]/[H^+]^2)$ terms essentially depict the pH changes of samples. Similarly, the same

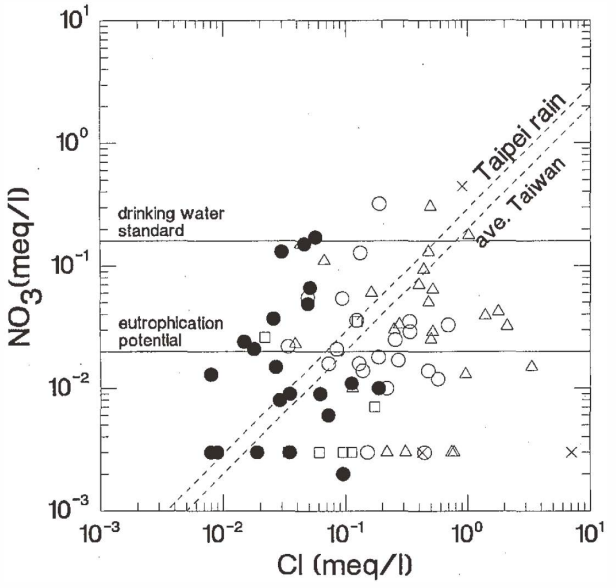

Fig. 10. Concentrations of Cl against nitrate in lakes and reservoirs. The dotted lines represent the NO_3/Cl ratios of the average and polluted Taipei rainwaters (Table 1). The horizontal lines are the nitrate drinking water standard and nitrate concentration for potential lake eutrophication as indicated.

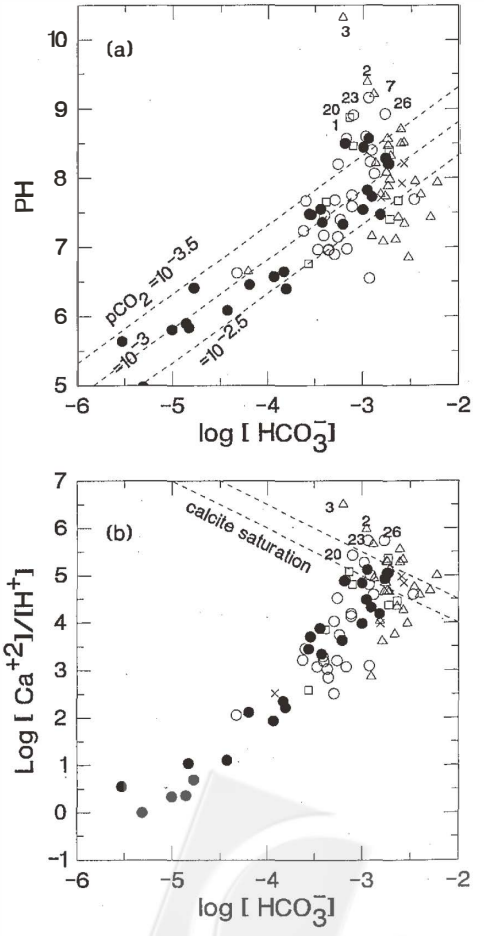

Fig. 11. (a) Plot of bicarbonate activities vs. pH. The dotted lines are equation 2 in the text with given Pco_2 values. (b) Plot of bicarbonate activities vs. the activity ratio of calcium and hydrogen ions. The calcite saturation line from equation 3 is also given. Numerals are specific sample numbers given in Table 1.

conclusion can be derived for Figure 12b. This means that there is no need to invoke Norton's (1974) notion that Ca, Mg and Na are released from solid phases into river waters in equal molar concentrations at equilibrium conditions.

3.5 Classification Scheme of Natural Waters by Gibbs

In the plots of the total dissolved salts versus the weight ratios of Na/(Na +Ca) and Cl/ ($Cl+HCO_3$) (Figure 13), the chemical data of numerous rivers and lakes around the world (Livingstone, 1963) mostly fall within the fields enclosed by the dashed lines (Gibbs, 1970). The waters with low dissolved salts and high weight ratios of Na/(Na+Ca) and Cl/($Cl+HCO_3$) reflect dominant sources of atmospheric precipitation (referred to as being rain-dominated). Increasing Ca and HCO_3 inputs from the chemical weathering of surficial rocks produce waters with low weight ratios of Na/(Na +Ca) and Cl/($Cl+HCO_3$) and moderate contents of total dissolved salts (also referred to be rock-dominated). Further evaporation of water and concurrent precipitation of $CaCO_3$ produce waters with high dissolved salts and high weight ratios of

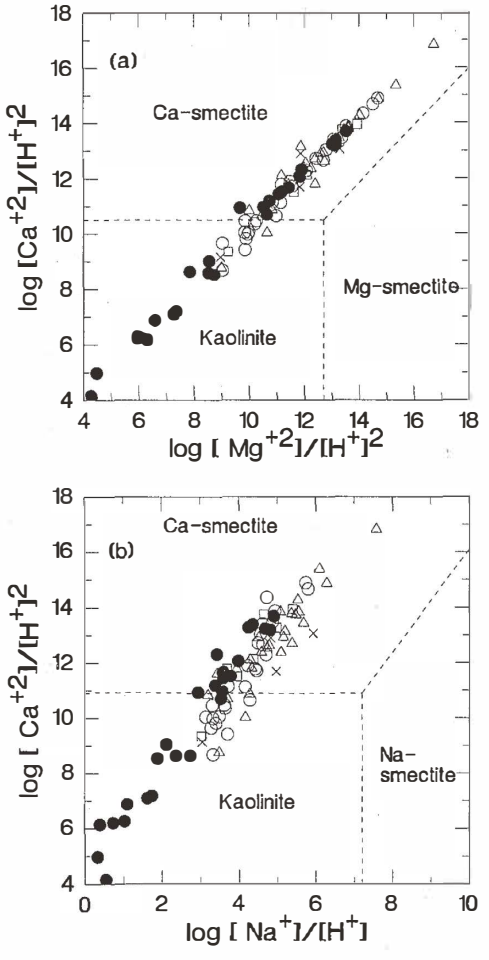

Fig. 12. Activity - activity diagrams and stability fields of Ca-, Mg- and Na-smectite and kaolinite.

Na/(Na+Ca) and Cl/(Cl+HCO_3) (also referred to be evaporation-crystallization dominated; Gibbs, 1970). As shown in Figure 13, most of the data from Taiwan's lakes and reservoirs similarly do fall within those fields, especially within the rain-dominated and rock-dominated segments. The obvious exception is the following: about one half of the mountain samples (solid circles in Figure 13a and b) tend to have low dissolved salts as compared to the coastal samples and to the world-wide surface waters at the given Na/(Na+Ca) and Cl/(Cl+HCO_3) values. As stated earlier, this fact can be explained both by the wash-out of a large fraction of seasalt aerosols before reaching the high mountain area and by the dilution effect of seasalt by high rainfall in this high mountain area.

Even though most of the coastal samples from Taiwan fall within the fields of world-wide surface waters, their rain-dominated segment tends to have high dissolved salts (n1, n4, and s27 in Figure 13), reflecting the high dissolved salts in the local coastal rainwaters (Table 1, and the open stars in Figure 13). Samples s3, s5, s14, s29, i1 and i13 (enclosed by the dotted line in Figure 13) fall outside the field of world-wide surface waters, especially with respect to Na/(Na+Ca) ratios (Figure 13a). Again this indicates appreciable Na inputs from chemical weathering of feldspars and Na-rich plagioclase.

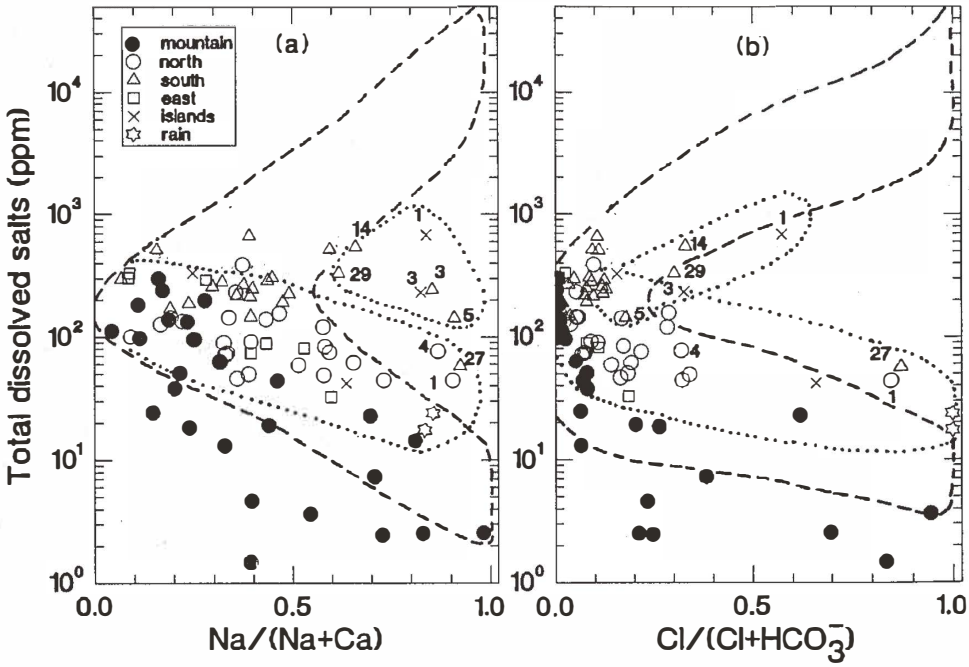

Fig. 13. Plots of the total dissolved salts versus the weight ratios of Na/(Na + Ca) and Cl/(Cl + HCO_3) for the world-wide surface waters (fields enclosed by dashed lines, given by Gibbs, 1970), and for water samples from Taiwan's lakes and reservoirs. The dotted lines enclose normal coastal samples and some unusual samples discussed in the text. Numerals are specific sample numbers given in Table 1.

Finally, the ratio of a given pair of elements for the world mean river water is shown as a solid diagonal line in each diagram of Figure 8 and 9. The data from Taiwan's lakes and reservoirs more or less cluster along those solid diagonal lines. Therefore, despite the exceptionally high chemical weathering rates of the island, the chemical weathering products from Taiwan are not much different from those of other areas around the globe (Li, 1976).

4. SUMMARY AND CONCLUSIONS

(1) Systematic variations in the chemical composition of for lake and reservoir waters from Taiwan as functions of distance from the coast (Figure 6) and altitude (Figure 7) can be explained by three factors: (i) the diminishing seasalt inputs from coastal to high mountain areas; (ii) the inputs from chemical weathering of carbonate and silicate rocks in upstream drainage areas of lakes and reservoirs; and (iii) the dilution by high rainfall in the high mountain areas, and evaporative concentration in coastal areas, especially along the southwestern coast of Taiwan.

(2) The close correlations among the concentrations of Ca, Mg, Alk and SO_4 are best explained by the chemical weathering of marble, gneiss and schists in the Central Range of Taiwan, which also contains chalcopyrite and pyrite veins and ores. Large fractions of Na and K in lake and reservoir waters are also the end products of chemical weathering.

(3) High mountain lakes with low alkalinity may be susceptible to acidification by acid rains. The extremely high chemical weathering rates in the Central Range, on the other hand, may mitigate acidification.

(4) The Pco_2 values of water samples as calculated from pH and alkalinity values (Figure 11a) are mostly greater than the atmospheric Pco_2, indicating active microbial oxidation of organic matter in lakes and reservoirs. A few coastal samples have calculated Pco_2 values much lower than the atmospheric Pco_2, probably caused by active photosynthesis in the water bodies, and become oversaturated with respect to calcite. Otherwise, most of the water samples are under-saturated to saturated with respect to calcite (Figure 11b).

(5) The activity-activity diagrams (Figure 12) indicate that kaolinite is a stable secondary clay mineral in high mountain (> 2000 m) lakes and reservoirs, whereas Ca-smectite and/or kaolinite are stable secondary clay minerals in the other lakes and reservoirs. The observed 1:1 and 2:1 slopes in Figures 12a and 12b are shown to be artifacts.

(6) In spite of exceptionally high chemical weathering rates in Taiwan, the compositions of water samples from Taiwan's lakes and reservoirs are mostly comparable to those of the world-wide surface waters (Livingstone ,1963; and Gibbs, 1970). Exceptions are some mountain samples which tend to have low dissolved salts relative to the world-wide surface waters due to the wash-out of seasalt aerosols before reaching to the high mountain areas (Figure 13). Additionally, some coastal samples have unusually high Na/(Na+Ca) values when compared with the world-wide surface waters at moderate total dissolved salt concentrations; they also show low $Cl/(Cl+HCO_3)$ values (Figure 13), suggesting Na inputs from the chemical weathering of Na-rich minerals, such as feldspars and plagioclases.

Acknowledgments This work is supported by the National Science Foundation grant number INT94-17480 to YHL, and by the National Science Council (NSC82-0209-M110-041)

and the Environmental Protection Administration (EPA82-G104-09-12) to CTC and JJH. Acknowledgment is also due to two anonymous reviewers. This is SOEST publication number 4567.

REFERENCES

Bluth, G J. S., and L. R. Kump, 1994: Lithologic and climatologic controls of river chemistry. *Geochim. Cosmochim. Acta* **58**, 2341-2359.

Central Weather Bureau, 1991: *Atlas of Climate in the Taiwan Region*. vol. 1, Ministry of Transportation (Taiwan), (in Chinese).

Chen, C. T. A., J. J. Hung, and B.J. Wang, 1988: The past, present and future of lake acidification in Taiwan. Inst. of Marine Geology, National Sun Yat-Sen Univ. Technical Report #2, pp 131 (in Chinese).

Chen, C. T. A., 1994: Effect of acid rain on lake acidification in Taiwan. Inst. of Marine Geology, National Sun Yat-Sen University, Technical Report #21. 77 pp (in Chinese).

Chen, C. T. A., B. J. Wang, Hsu H. C., and J. T. Hung, 1994: Rain and lake waters in Taiwan: Composition and acidity. *TAO* **4**, 573-584.

Colman, S. M., 1982: Chemical weathering of basalts and andesites: Evidence from weathering rinds. USGS Prof. Paper 1246. Washington, D.C.

Degens, E. T. editor, 1982: Transport of Carbon and Minerals in Major World Rivers, Part 1. SCOPE/UNEP International Carbon Unit, University of Hamburg.

Degens, E. T., S. Kempe, and M. Soliman editors, 1983: Transport of Carbon and Minerals in Major World Rivers, Part 2. SCOPE/UNEP International Carbon Unit, University of Hamburg.

Degens, E. T., S. Kempe, and R. Herrera editors, 1985: Transport of Carbon and Minerals in Major World Rivers, Part 3. SCOPE/UNEP International Carbon Unit, University of Hamburg.

Drever, J. I. editor, 1985: The Chemistry of Weathering. D. Reidel Publ. Co.

Drever, J. I., 1988: The Geochemistry of Natural Waters. Prentice-Hall, New Jersey.

Gibbs, R. J., 1970: Mechanisms controlling world water chemistry. *Science* **170**, 1088-1090.

Ho, C. S., 1975: An Introduction to the Geology of Taiwan. Ministry of Economic Affairs, Republic of China. 153 pp.

Konishi, K., A. Omura, and T. Kimura, 1968: U^{234} - Th^{230} dating of some late Quaternary coralline limestones from southern Taiwan (Formosa). *Geol. and Pal. of Southeast Asia* **5**, 211-224.

Lan, C. Y., T. Lee, S. A. Mertzman, T. W. Wu, B. M. Jahn, T. F. Yui, and J. S. Shen, 1991: Geochemical and isotopic study of gneiss, associated metabasites at the Central Range, *Taiwan. Prod. Geol. Soc. China (Taiwan)* **34**, 233-266.

Lerman, A., D. Imboden, and J. Gat editors, 1995: Physics and Chemistry of Lakes. Springer-Verlag.

Li, Y. H., 1972: Geochemical mass balance among lithosphere, hydrosphere and atmosphere.

Am. J. Sci. **272**, 119-137.

Li, Y. H., 1976: Denudation of Taiwan Island since the Pliocene Epoch. *Geology* **4**, 105-107

Li, Y. H.,1988: Denudation rates of the Hawaiian Islands by rivers and groundwaters. *Pacific Science* **42**, 253-266.

Li, Y. H.,1992: Seasalt and pollution inputs over the continental United States. *Water, Air and Soil Pollution* **64**, 561-573.

Liew, P. M., Hsieh M. L., and Lai C. K., 1990: Tectonic significance of Holocene marine terraces in the Coastal Range, eastern Taiwan. *Tectonophysics* **183**, 121-127.

Liu, C. C., and Yu S. B., 1990: Vertical crustal movements in eastern Taiwan and their tectonic implications. *Tectonophysics* **183**, 111-119.

Livingstone, D. A., 1963: Chemical composition of rivers and lakes, in Data of Geochemistry, 6 th ed. by M. Fleischer, U.S. Geol. Surv. Prof. Paper, 440-G.

McCabe, L. J., Symons, J. M., Lee, R. D., and Robeck, G. G., 1970: Survey of community water supply systems. *J. Am. Water Works Assoc.* **62**, 670-687.

Meybeck, M., 1987a: How to establish and use world budgets of river material. in Physical and Chemical Weathering in Geochemical Cycles. eds. Lerman A. and Meybeck M. NATO ASI series, Kluwer Acad. Publ. 247-272.

Meybeck, M., 1987b: Global chemical weathering of surficial rocks estimated from river dissolved loads. *Am. J. Sci.* **287**, 401-428.

Norton, D., 1974: Chemical mass transfer and the Rio Tanama system, west-central Puerto Rico. *Geochim. Cosmochim. Acta* **38**, 267-277.

Peng, T.H., Li Y.H., and Wu F.T., 1977: Tectonic uplift rates of the Taiwan Island since the early Holocene. Memoir Geol. Soc. China (Taiwan) no.**2**, 57-69.

Sawyer, C. N., 1947: Fertilization of lakes by agricultural and urban drainage. *J. New Engl. Water Works Assoc.* **61**, 109-127.

Schindler, D. W., 1974: Experimental studies of eutrophication and lake recovery: Some implications for lake management. *Science* **184**, 897-899.

Schindler, D. W., 1977: Evolution of phosphorus limitation in lakes. *Science* **195**, 260-262.

Stallard, R. F., and Edmond J. M., 1981: Geochemistry of the Amazon 1, Precipitation chemistry and the marine contribution to the dissolved load at the time of peak discharge. *J. Geophys. Res.* **86**, 9844-9858.

Stallard, R. F., and Edmond J. M., 1983: Geochemistry of the Amazon 2, The influence of geology and weathering environment on the dissolved load. *J. Geophys. Res.* **88**, 9671-9688.

Stallard, R. F., and Edmond J. M., 1987: Geochemistry of the Amazon 3, Weathering chemistry and limits to dissolved inputs. *J. Geophys. Res.* **92**, 8293-8302.

Stumm, W. editor, 1985: Chemical Processes in Lakes. John Wiley & Sons, New York.

Vollenweider, R. A., 1975: Input and output models. Schweiz. Z. Hydrol. 37, 53-84.

Wang, J. I., and Yi J., 1992: Applied Hydrology. National Office of Translation (Taiwan), (in Chinese).

Wang, C. H., and Burnett W.C., 1990: Holocene mean uplift rates across an active plate-collision boundary in Taiwan. *Science* **248**,204-206.

Wang, H., 1980: Topographic Scenery of Taiwan. Holiday Publ. Co. Taipei (in Chinese) .